

Experimental Evaluation of Adaptive Maximum PowerPoint Tracking for a Standalone Photovoltaic System

Ihechiluru Anya · Chitta Saha · Hafiz
Ahmed · Sujan Rajbhandari · Nazmul
Huda · Asim Mumtaz

Received: date / Accepted: date

Abstract The adaptability of maximum power point tracking (MPPT) of a solar PV system is important for integration to a microgrid. Depending on what fixed step-size the MPPT controller implements, there is an impact on settling time to reach the maximum power point (MPP) and the steady state operation for conventional tracking techniques. This paper presents experimental results of an adaptive tracking technique based on Perturb and Observe (P&O) and Incremental Conductance (IC) for standalone Photovoltaic (PV) systems under uniform irradiance and partial shading conditions. Analysis and verification of measured and MATLAB/Simulink simulation results have been carried out. The adaptive tracking technique splits the operational region of the solar PV's power-voltage characteristic curve into four and six operational sectors to understand the MPP response and stability of the technique. By implementing more step-sizes at sector locations based on the distance of the sector from the MPP, the challenges associated with fixed step-size is improved on. The measured and simulation results clearly indicate that the proposed system tracks MPP faster and displays better steady state operation than conventional system. The proposed system's tracking efficiency is over 10 % greater than the conventional system for all techniques. The proposed system has been under partial shading condition has been and it outperforms other techniques with the GMPP achieved in 0.9s which is better than conventional techniques.

Keywords Solar · Perturb and Observe (P&O) · Photovoltaic (PV) · Incremental Conductance (IC) · MPPT

Ihechiluru Anya
School of Computing, Electronics and Mathematics, Coventry University, Priory Street,
Coventry CV1 5FB, UK
Tel.: +447799832982
E-mail: anyai@uni.coventry.ac.uk

1 Introduction

Global energy demand is growing rapidly as the industrial sector increases as well as increase in transport, commercial and residential demand. Conventional energy sources which include fossil fuels, petroleum, etc. are rapidly declining and greatly contributing to the menace of climate change and global warming. These developments have motivated countries and energy companies to explore alternative sources of energy [1]. Electrical energy derived from renewable sources have provided an efficient way to manage the challenges. Electrical energy derived from renewable sources is responsible for 40 % of the global energy growth and is consistently growing [2–4]. The benefits of solar energy are significant and when compared to other sources, it exhibits the least harmful effect on the environment. However, it faces the challenge of high initial cost and poor conversion efficiency (9-17 %) due to material intrinsic properties, solar irradiance and temperature conditions [5–8]. Recent trends from ongoing research show an improved efficiency of over 25 % [9]. To address this challenge it is necessary to develop new high efficient solar PV materials. Alternatively, a viable solution is to improve the efficiency of light to electrical energy conversion through the implementation of a sun tracking system [10, 11]. The solar PV power-voltage (P-V) characteristic curve is non-linear and changes based on the applied load condition and test conditions on the solar panel. The MPP at the P-V characteristic curve is unknown, however, it can be identified easily by implementing tracking methods. The direct methods include perturb and observe (P&O), incremental conductance (IC) [12–14] and the indirect methods include particle swarm optimization(PSO), fraction short circuit current, fuzzy logic, fraction open circuit voltage [15–18], etc. Existing algorithms have various benefits and drawbacks bordering on speed of convergence to MPP, complexity and cost.

Practically, the most common tracking methods are the P&O and IC due to their simple operation. They require few sensors which reduce their overall cost in contrast to other techniques. Under the P&O method, perturbation is provided to the PV voltage to cause an increase or decrease in power. An increase in power due to voltage increase implies that the operating point is to the left of the MPP, therefore, further voltage perturbation is required towards the right to move the operating point towards the MPP. Alternatively, a decrease in power due to voltage increase implies that the operating point is to the right of the MPP, therefore, further voltage perturbation is required towards the left to move the operating point towards the MPP. Under the IC method, the MPP is achieved when the slope of the P-V curve is zero. Voltage is imposed on the PV module at every iteration, the incremental change in conductance is measured and compared to the instantaneous conductance, the algorithm then decides if the operating point is to the left or to the right of MPP and the appropriate action is executed [19, 20]. Conventionally, the MPPT controller implements a fixed step-size to track MPP. The MPP can be achieved more rapidly by implementing a large step-size, however, more oscillations will exist at steady state operation. With the implementation of

a small step-size, MPP can be achieved with low oscillations at steady state operation, however, a longer time would be taken to achieve MPP [21, 22]. The IC tracking method when compared to the P&O has the advantage of less oscillations at steady state operation [23, 24]. To enhance the performance of these tracking methods under uniform irradiance condition (UIC), several alternatives have been presented. For example, Ghassami *et al.* [25] proposes modified P&O and IC MPPT algorithms by using the I-V curve to adjust MPP operating point. It displays the drawbacks associated with the conventional system and it improves on the tracking properties of the conventional system. In [26], Ganesh *et al.* proposes an adaptive conductance ratio algorithm by implementing a PI controller to obtain suitable duty cycle to enhance steady state operation and time to attain MPP. A hybrid MPPT algorithm [27], made up of P&O and IC tracking methods has been implemented using variable step-size to enhance the time to track MPP and reduce oscillations around MPP but does not account for shading conditions in the system. In [28], 4 sector P&O MPPT implementation has been executed to improve the settling time at MPP and steady state operation under uniform irradiance condition, step-changing irradiance condition and fast changing irradiance condition.

However, under partial shading condition (PSC), conventional MPP techniques do not perform effectively because the P-V characteristic curve exhibits multiple peak power points [29]. In this case, global maximum power point (GMPP) based tracking method could be a suitable option to extract GMPP from multiple peak values efficiently and reliably. GMPP can be obtained by implementing a dc power optimizer which is a specially designed converter with a separate controller [30], by modifying conventional MPPT methods, or combining different methods to avoid the local maximum power points (LMPPs) which can solve the challenge posed by partial shading condition (PSC). For example, Alonso *et al.* [31] presents a modified P&O MPPT algorithm that implements P&O at certain areas on the basis of bypass diodes technique to extract the GMPP successfully. In their technique, the different maximum power points at P-V characteristic curves can be observed but there is no justification for choosing the certain areas provided in the paper. The work presented by Sundareswaran *et al.* [32] is a hybrid made up of P&O and Genetic Algorithm to improve settling time at MPP and steady state operation with the evaluation of chromosomes (duty cycles). They have used three iterations and the appropriate duty cycle at starting by the P&O MPPT which employs an adaptive technique to increase convergence time. In spite of the good performance of the system, its application is limited to certain shading patterns. In [33], a hybrid technique made up of P&O and PSO is presented and their approach adjust the first maximum operating point by P&O which will ultimately reduce the search area and the convergence time while Jiang *et al.* [34] proposes a hybrid combination of P&O and ANN to successfully track GMPP in which the ANN predicts the scanning area for the GMPP and P&O tracks the GMPP. The fuzzy logic control (FLC) algorithm for MPPT in [35] uses three fuzzy rules and linguistic variables based on reference power by tracking the GMPP to improve the computational time as well as convergence

time. Also, Sundareswaran *et al.* [36] presented a hybrid made up of P&O and PSO algorithms where the convergence quality of P&O and the global search quality of the swarm intelligence are integrated to successfully track GMPP.

A significant amount of research has been published for MPPT and most of the prior research in Solar MPPT discusses the different step-sizes and investigates the computational efficiency based on the simulation result without verification of simulation with experimental values. Also, most of the published works have investigated the efficiency of the solar PV system under standard test condition and non-uniform irradiance condition. This paper presents an adaptive MPPT algorithm for a standalone system that is implemented using a variable voltage step-size to improve the overall system performance under standard test condition and partial shading condition. The hardware prototype of P&O and IC techniques has been set up and the measured results have been analyzed with theory and MATLAB/Simulink simulation. Finally, this research work is compared and some conclusions are drawn with the published works. The structure of this paper is as follows; Section 2 gives a background theory of solar PV and MPPT. Section 3 discusses the test set up of the hardware. Section 4 describes the proposed MPPT algorithm. In section 5, analysis and discussion of the measured and simulated results are provided. The conclusion is presented in section 6, including key achievements from this work and future areas of investigation.

2 Background theory of Solar PV and MPPT

Many models exhibit the characteristics of solar cells, however, in application the commonly utilized models are the one diode, the double diode and the triple diode equivalent circuit models. In this paper, the one diode model is considered due to its computational simplicity and accuracy in defining the P-V curve of a module for a given set of working conditions. Also, the accuracy of the power generated by each PV cell has no impact on the ability of the maximum power point tracking technique. The one diode output current of the PV module can be expressed as shown in Eq.(1) [37].

it would not change the final result as the accuracy of the power generated by each PV cell has no impact on the ability of the maximum power point tracking technique so emphasis is not on generating accurate power but on extracting the maximum power from the generated power

$$I = I_L N_2 - I_{RS} N_2 \left[\exp \left(\frac{q \{I R_s + V_{pv}\}}{N_1 T A K} \right) - 1 \right] \quad (1)$$

Where N_1 represents strings connected in series, I_{RS} stands for diode reverse saturation current, N_2 represents strings connected in parallel, R_s for series resistance, K for boltzmann's constant, I_L is the current generated from light, A for diode ideality factor, and V_{pv} is the output voltage of solar PV. The Irradiance, G and Temperature, T influence the light generated current, I_L . Further details of all parameters for Eq.(1) can be found in [37].

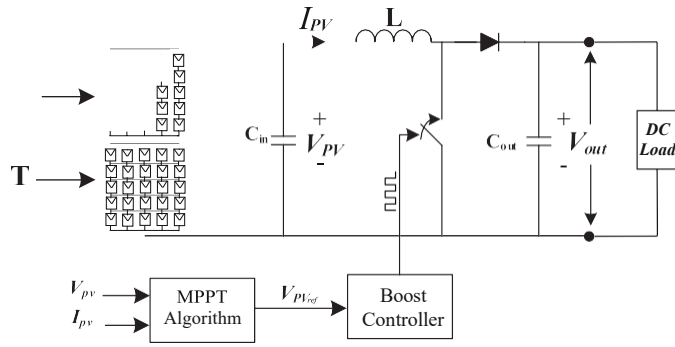


Fig. 1: Electrical circuit block diagram of Solar PV system.

The electrical circuit block diagram of the solar PV integrated with a boost converter (BC) and load is shown in fig. 1. The BC is an intermediary between the solar PV and load which is capable of stepping up the solar PV voltage, (V_{pv}) to a certain output voltage, (V_{out}). The duty cycle, D regulates the required V_{out} .

$$V_{out} =$$

The proper justification for MPPT operation is that at the peak of the P-V characteristic curve, the change in the solar PV output power is zero ($\Delta P_{pv} = 0$). The P&O tracking method functions by regularly perturbing the solar PV output voltage and current and relating the resultant power $P_{(n+1)}$ to the resultant power $P_{(n)}$ of the previous perturbation.

The IC tracking method functions such that the derivative of the solar PV power to the voltage is zero ($\frac{\Delta P}{\Delta V} = 0$). It is negative to the right of MPP and positive to the left. The MPP is attained when the the derivative of the solar PV current to the voltage ($\frac{\Delta I}{\Delta V}$) is equal to the change in current with respect to voltage ($\frac{I}{V}$). The MPP operation is maintained except a change in current, ΔI is observed thus, indicating alteration in test conditions resulting to a change in MPP. Therefore, the IC MPPT operation increases and decreases the voltage to attain MPP.

3 Experimental Test Setup

Fig. 2 shows the practical set up of the solar PV system implementation. The setup is made up of three main elements; EA Elektro-Automatik PSI 9360-30 solar simulator, C2000 Microcontroller unit designed by Texas Instrument and an EA Elektro-Automatik electronic load. The PSI 9360-30 solar simulator emulates the P-V characteristics of a PV panel and the microcontroller unit is a digitally Controlled HV Solar MPPT Converter. The voltage and

current are measured by the PINTEK DP-25 sensor and the Chauvin Arnoux P01120043A sensor respectively. Using solar software libraries the modified MPPT algorithms can be implemented in the C2000 Piccolo MCU.

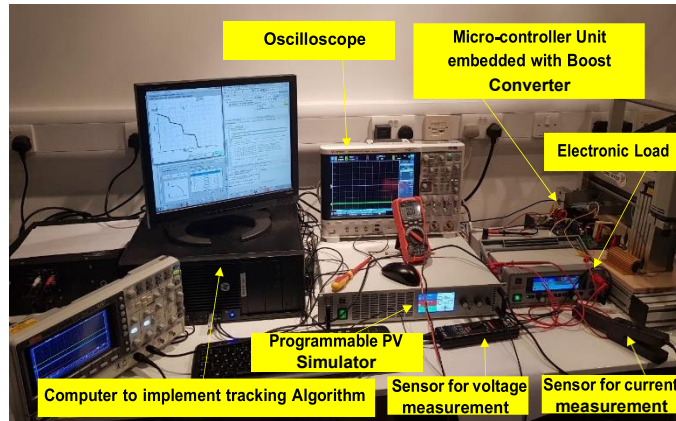


Fig. 2: MPPT Hardware Implementation Setup.

Table 1: Characteristics of solar PV system.

Power Rating at MPP	165 W
Voltage Rating at MPP	220 V
Current Rating at MPP	0.75 A
Rated Open Circuit Voltage	260 V
Rated Short Circuit Current	1 A

The voltage and current range of the MPPT algorithm are defined by the measured V_{out} and I_{out} of the solar PV. The PV system generates a voltage, V_{pv} and current, I_{pv} of 220 V and 0.75 A respectively. The voltage is supplied to the BC of the microcontroller unit and is stepped up to a V_{out} of approximately 403 V. The microcontroller unit regulates the BC signal by using 4 PWM and 3 feedback signals. The PWM signals reduce the solar PV's ripple current while the feedback signals help to carry out the control loops for the BC. The implemented MPPT technique ensures a voltage reference, V_{ref} of the solar simulator output voltage, V_{pv} is set and this is done by a control system which regulates the V_{pv} around the V_{ref} . The BC's output is connected to an electronic load which pulls a current of 0.41 A. Table 1 shows the solar PV's characteristics under uniform irradiance of 1000 Wm^{-2} and an ambient air temperature of $25 \text{ }^\circ\text{C}$.

4 Sector modified MPPT

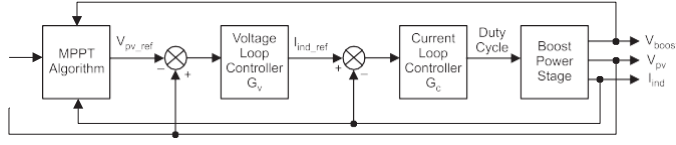


Fig. 3: MPPT BC Control Loops.

Extraction of power from solar PV system is critical in microgrid integration and application. Hence, the development of a fast, robust and efficient MPPT control technique is significant to achieve MPP. This will enhance solar PV system performance and efficiency for different operating conditions. Fig. 3 shows the proposed MPPT control loop and this control loop process is implemented in conjunction with the MPPT algorithm in the microcontroller unit using a separate solar library function. The aim is to control the PV panel output voltage (V_{pv}). The MPPT algorithm sets a reference voltage (V_{pvref}) and V_{pv} is compared with V_{pvref} . The resultant error signal (E_v) is the input to the voltage loop controller (G_v). G_v controls the voltage of the PV panel according to the set reference. The output from G_v is the reference current (I_{indref}) for the inductor current loop. I_{indref} is then compared with feedback inductor current (I_{ind}). The resultant error signal (E_c) is the input to the current loop controller (G_c). G_c controls the current of the PV panel and generates a duty cycle for the switches. In order to operate a better efficient system and minimize power loss in the system, it is beneficial to use low power sensors as the amount of sensors influence the measurement complexity, overall losses and cost of the system [38].

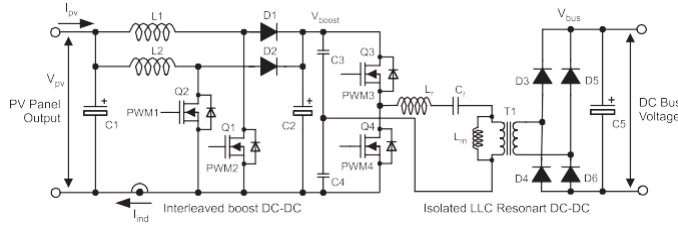


Fig. 4: MPPT BC Control Circuit Using C2000 MCU.

Fig. 4 shows the MPPT control system circuitry. This architecture enables rapid and accurate sensing, specialized processing to minimize latency and guarantees precise configurable actuation. From the circuit, V_{out} is connected

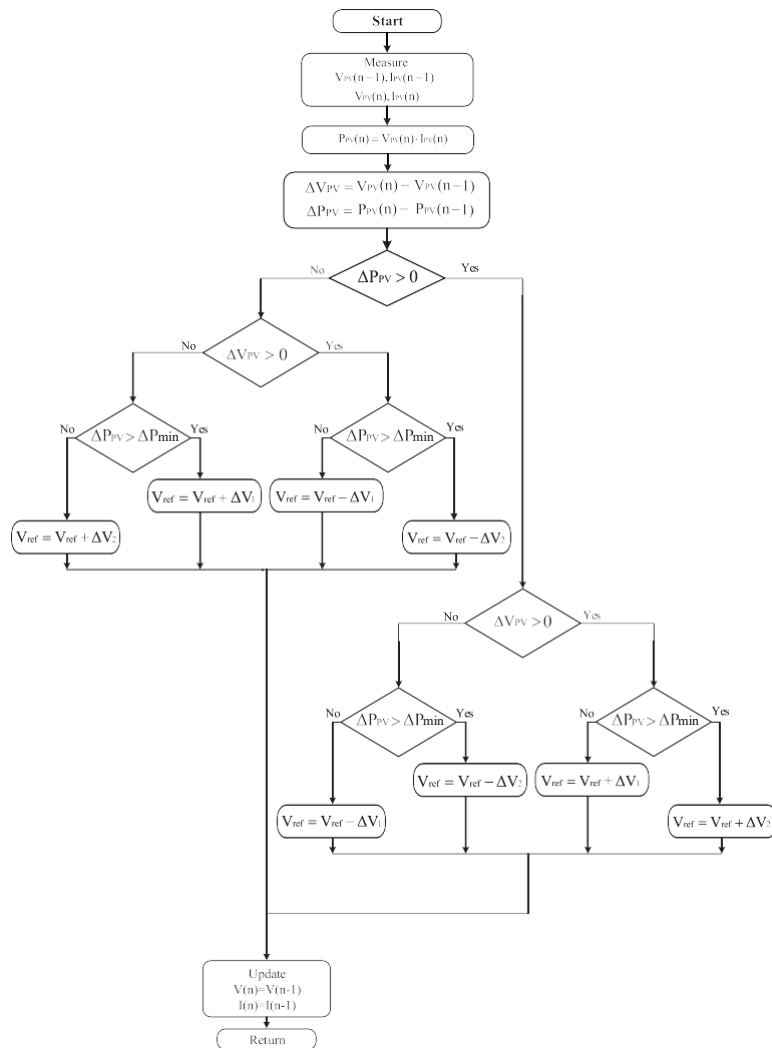


Fig. 5: FlowChart of the proposed MPPT technique.

to the 2 phase interleaved boost stage. One phase is formed by L_1 , D_1 and Q_1 and another phase by L_2 , D_2 and Q_2 . The control loop is designed by feeding back sensed signals ((V_{pv}) , BC output voltage (V_{con}) and current (I_{con})) to the microcontroller unit. The duty cycles of switch Q_1 and Q_2 control the input current which also controls the input voltage. Fig. 5 illustrates the flow chart for the proposed model. The sector modified technique like the conventional technique relies on the identification of the point of operation on the P-V characteristic curve. A new curve, $(G_{\frac{dP}{dV}})$ is combined with the characteristic curve to split the operating region into multiple sectors. Fig. 6 shows a four

sector division of the characteristic curve while Fig. 7 shows a six sector division of the characteristic curve in order to reduce the oscillations at steady state operation the sectors.

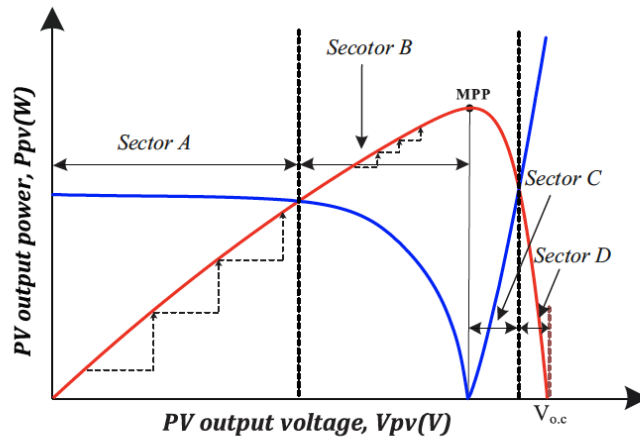


Fig. 6: Four sector MPPT concept.

For the four sector division, a small step-size is applied at sectors B and C otherwise large step-size is employed (sectors A and D). For the six sector division, a smaller step-size is applied at sectors B2 and C2, the small step size is applied at B1 and C1 and large step-size is applied at sectors A and D.

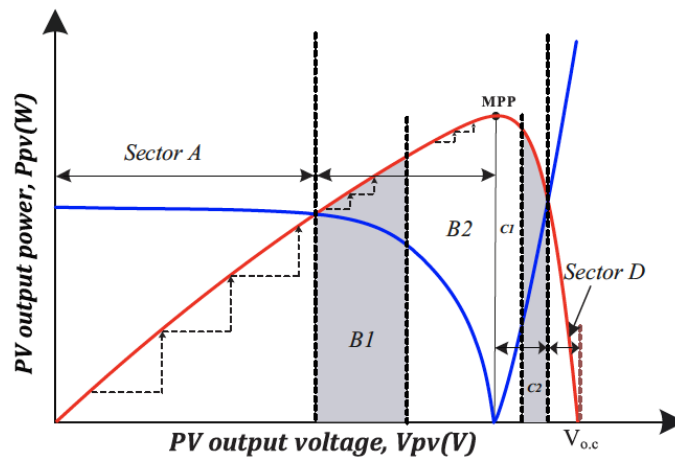


Fig. 7: Six sector MPPT concept.

MPPT is implemented to the BC and two fundamental configurations can be used to control the switching process of the BC and achieve perturbation. This can be perturbation of D or perturbation of V_{ref} which generates a signal to control the D . The general equation describing the size of perturbation is as expressed in Eq.(3) adopted from [39]

$$\begin{aligned} x_{((k+1)T_p)} &= x_{(kT_p)} \pm \Delta x \\ &= \{x_{(kT_p)} + (x_{(kT_p)} \end{aligned}$$

As described, fixed step-size is implemented by conventional tracking methods, $\Delta x = x_{(kT_p)} - x_{((k-1)T_p)}$. Where x represents the perturbed voltage reference, Δx is the step-size on x , T_p is the time in the middle of perturbations and P is the solar PV power. Variable step-size is implemented according to point of operation to improve performance by relating to the derivative of power with the derivative of voltage (dP/dV). Eq.(3) is modified as follows;

$$x_{((k+1)T_p)} = x_{(kT_p)} \pm \Delta x = x_{(kT_p)} \pm N \frac{|P_{(kT_p)} - P_{((k-1)T_p)}|}{|V_{PV(kT_p)} - V_{PV((k-1)T_p)}|} \quad (4)$$

Where N as the scaling factor is modified to control the step-size. (dP/dV) adjusts the D of the BC to enhance the settling time at MPP and steady state operation. By implementing average state space modelling to the implemented converter design, the complete transfer function expression is obtained as shown in Eq.(5).

$$G_{vp,x}(s) = \frac{\widehat{v}_{pv}(s)}{\widehat{x}(s)} = \frac{\mu \cdot \omega_n^2}{s^2 + 2\zeta \cdot \omega_n \cdot s + \omega_n^2} \quad (5)$$

Where ω_n is the natural frequency, μ is the static gain and ζ is the damping factor [39–41]. \widehat{v}_{pv} and \widehat{x} represent small-signal voltage and power changes at steady-state.

$$\widehat{v}_{pv}(t) = \mu \Delta x \left(1 - \right.$$

From the second-order transfer function, $G_{vp,x}(s)$, the response \widehat{v}_{pv} and \widehat{x} to perturbation of step-size Δx can be obtained. Based on the BC parameters, the values of μ , ω and ζ are defined. The response \widehat{v}_{pv} to perturbation can be expressed as Eq.(6) and the response \widehat{x} to perturbation can be approximated as Eq.(7);

$$\widehat{p}_{pv}(t) =$$

=

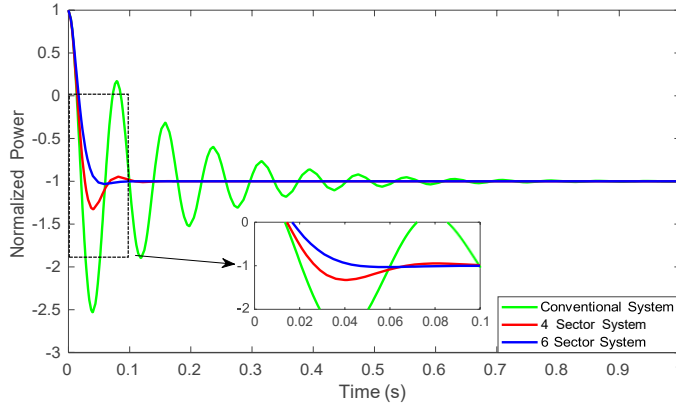


Fig. 8: Dynamic behaviour of PV power.

5 Results and discussion

Results have been presented for the implementation of conventional and sector modified tracking techniques for P&O and IC under uniform irradiance condition and partial shading condition. Analysis has been carried out using Eq.(3)-(7) to verify the impact of sector modification to the settling time at MPP and the system steady-state operation. Fig. 8 illustrates the results of normalized PV power oscillation from the implementation of the standard, 4 sector and 6 sector tracking techniques evaluated numerically using Eq.(7). By executing the condition in Eq.(8), the settling time T_ϵ can be introduced to ensure that the small-signal power variation \hat{p}_{pv} is limited inside a band of relative amplitude $\pm \epsilon$ around steady-state operation [39].

$$\hat{p}_{pv}(t) \in [\Delta P_f \cdot (1 - \epsilon), \Delta P_f \cdot (1 + \epsilon)] \forall t > T_\epsilon \quad (8)$$

Where ΔP_f is the final power variation due to the Δx . The settling time for the conventional system is 0.8 s, the 4 sector system is 0.09 s and the 6 sector system is 0.05 s. This validates the time to reach maximum power point in figs. 9, 10 and 11.

5.1 Uniform irradiance condition (UIC)

Fig. 9 illustrates MATLAB/Simulink simulation result for the solar PV system designed based on the control configuration of the microcontroller unit. The result show a high oscillation for the conventional system having a voltage of 10 V (peak to peak). The 4 sector modified system and 6 sector modified system show better voltage of 2 V and 0.5 V respectively (peak to peak). Also, the dynamic response for the sector modified system is much improved compared to the 800 ms of the conventional system. The 4 sector system

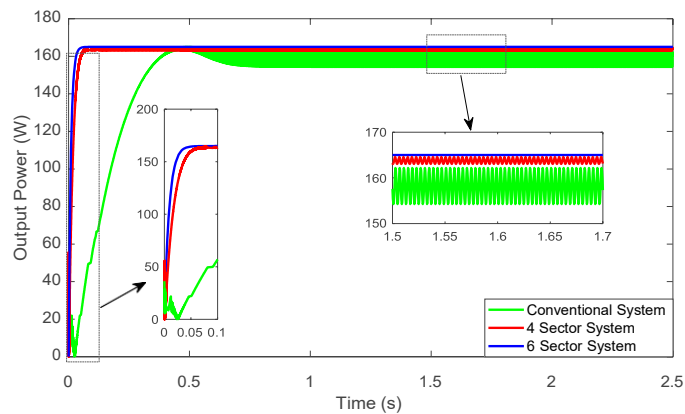


Fig. 9: Simulation result for P&O MPPT under UIC.

exhibits a dynamic response of 110 ms and the 6 sector system exhibits a dynamic response of 55 ms.

Figs. 10a and 10b shows measured results for conventional and sector modified techniques for the P&O MPPT. The controller also exhibits high oscillations for the conventional system with a voltage of 7 V (peak to peak) unlike the response of the sector modified system with a much improved voltage of 3 V (peak to peak). The dynamic response for the sector modified system is an improvement on the conventional system. However, the 4 sector system exhibits a dynamic response of 100 ms and the 6 sector system exhibits a dynamic response of 50 ms.

Table 2: Simulation and Measurement Comparison for different MPPT techniques.

MPPT Implementation	Voltage Ripple (V)	Step-size	Time to MPP (s)	Tracking Efficiency (%)
Con. Simulation	10.00		0.80	87.50
Con. P&O Measurement	7.00	$\Delta V_1=1e-2$	1.00	85.31
Con. IC Measurement	3.00		1.00	84.5
4 Sec. Simulation	2.00	$\Delta V_1=1e-2$	0.10	98.89
4 Sec. P&O Measurement	4.00	$\Delta V_2=1e-3$	0.10	97.36
4 Sec. IC Measurement	2.00		0.08	97.79
6 Sec. Simulation	0.50	$\Delta V_1=1e-2$	0.05	99.64
6 Sec. P&O Measurement	3.00	$\Delta V_2=1e-3$	0.05	98.75
6 Sec. IC Measurement	2.00	$\Delta V_3=1e-5$	0.06	98.22

Figs. 11a and 11b shows measured results for conventional and sector modified techniques for the IC MPPT. Generally, systems implementing incremental conductance display lower ripple content when compared with perturb and

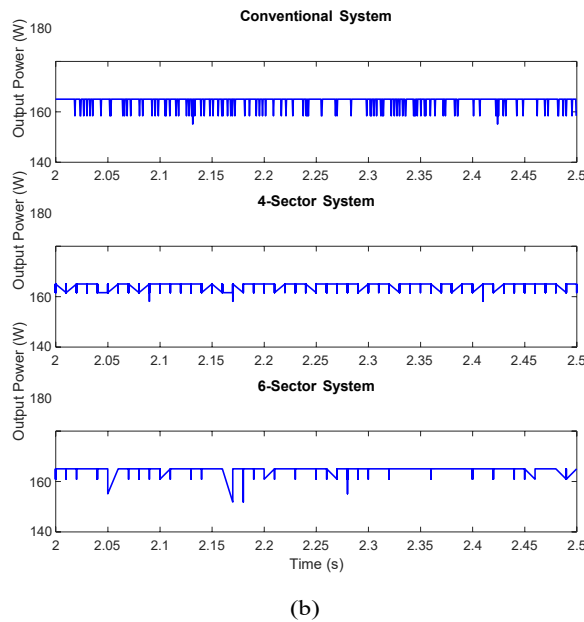
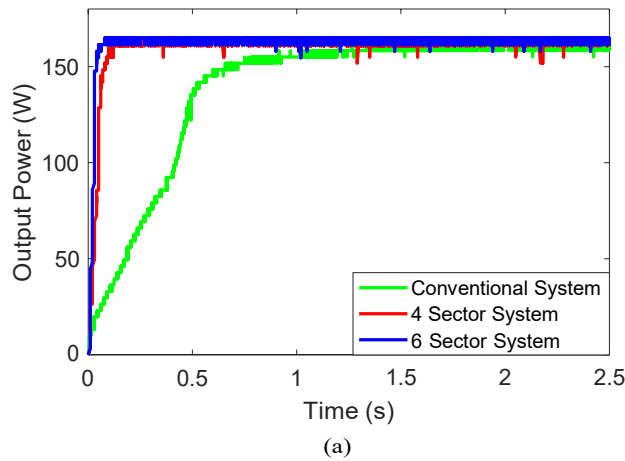
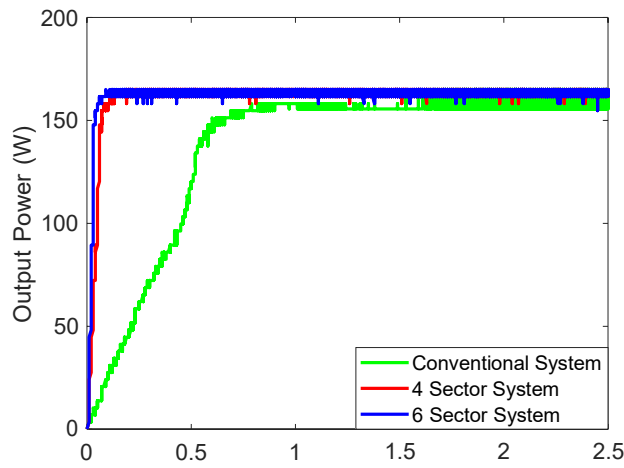
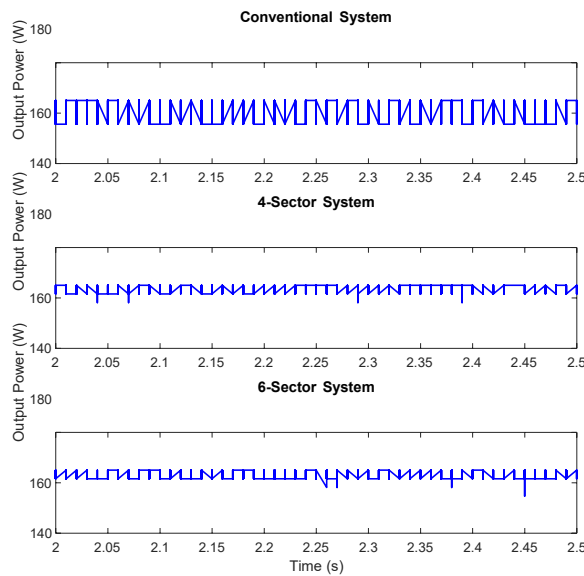


Fig. 10: Experimental result for P&O MPPT under UIC.

observe [42, 43]. The controller generally exhibits an average voltage of 3 V (peak to peak). The dynamic response for the sector modified system is an improvement on the conventional system. However, the 4 sector system exhibits a dynamic response of 60 ms and the 6 sector system exhibits a dynamic response of 40 ms. The above results validate the performance of the proposed system. After implementing the proposed technique, the system tracking efficiency increases from 85.31 % and 84.50 % to 98.75 % and 98.22 % for the conventional P&O and IC MPPT respectively. Table 2 summarizes the results of comparison between the conventional, 4 sector and 6 sector modified



(a)



(b)

Fig. 11: Experimental result for IC MPPT under UIC.

techniques. The sector modified system improves the dynamic response and reduces steady-state operation oscillations. Hence, it collaborates the advantages of both step-sizes and improves their challenges. Due to the nature of the 4 sector and 6 sector systems, the number of operations increases when compared to the conventional system, creating an increase in execution time. Consequentially, the computational complexity of the 4 sector and 6 sector systems is higher than the conventional system. However, there is a trade-

off between the computational complexity and efficiency of the system as the conventional system is less efficient than the modified 4 and 6 sector systems. Table 3 outlines the operations involved in implementing the conventional, P&O, and IC techniques.

Table 3: Operations involved in Implementing the different MPPT techniques.

	Average no of Iterations	Sectors Covered	No of step-sizes
Conventional System	5	2	1
4-sector System	8	4	2
6-sector System	13	6	3

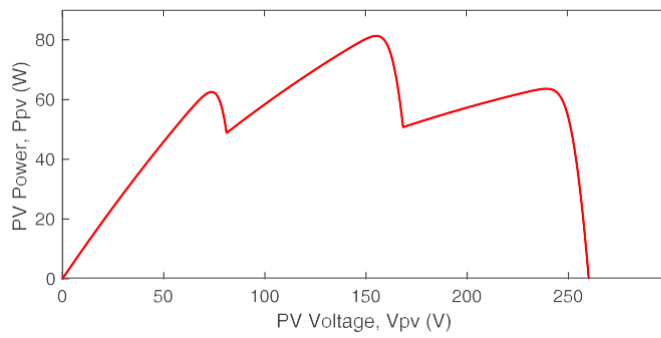


Fig. 12: PV Characteristic Curve under PSC for Case 1.

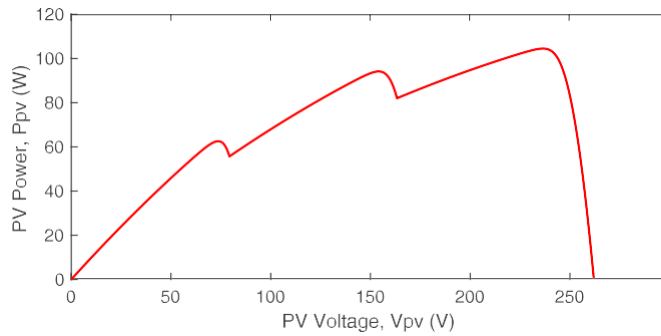


Fig. 13: PV Characteristic Curve under PSC for Case 2.

5.2 Partial shading condition (PSC)

Under partial shading condition, the performance of any solar PV whether standalone or grid-connected is considerably affected. The PV system, whether a module, string or array exhibits a PV characteristic curve possessing multiple peaks, a Global Maximum Power Point (GMPP) which is the highest maximum point and Local Maximum Power Points (LMPPs) which are multiple peaks. To ensure satisfactory performance under partial shading, the proposed MPPT identifies the GMPP. For GMPP Tracking, the BC output current, (I_{out}) and PV voltage, (V_{pv}) are significant are employed for identifying the MPP. The major GMPPT performance indicators are steady state oscillations, tracking speed and efficiency. As shown in figs. 12 and 13, the solar simulator emulates, two shading patterns to properly assess the efficiency of the proposed MPPT technique. The corresponding results are illustrated in figs. 14 and 15. It is evident that the P-V characteristic curve shows two peaks, the LMPP and GMPP. At GMPP, 80 W is delivered by the PV and 63 W is delivered at LMPP for case 1 and 100 W GMPP is delivered by the PV and 95 W is delivered at LMPP for case 2. From the result, the MPPT algorithm begins by identifying GMPP from the LMPP and then holds the GMPP that has been tracked. For both cases, the time taken to settle at GMPP is about 90 ms. The tracking efficiency produced for case 1 and case 2 are 99.5 % and 99.51 % respectively.

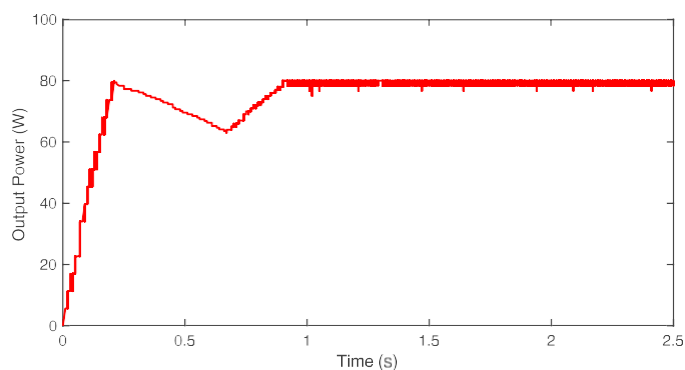


Fig. 14: GMPP under partial shading for Case 1.

Table 4 summarizes evaluation of the proposed system with existing system in [38, 44–46] with respect to number of sensors, steady state oscillations, tracking speed and efficiency under PSC. The proposed system displays a very good efficiency and time to settle at MPP (speed). The systems which display better settling time possess lower efficiency.

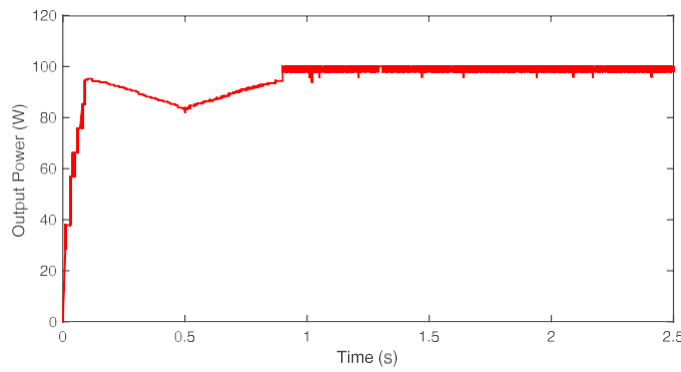


Fig. 15: GMPP under partial shading for Case 2.

Table 4: Comparison of Global MPPT performance for related systems.

Parameter	Sensors	Oscillation	Speed (s)	Efficiency (%)
[44]	2	Yes	1.20	99.60
[45]	2	No	5.00	99.00
[46]	2	Yes	2.50	99.25
[38]	2	Yes	0.12	97.00
[35]	2	Yes	0.50	98.50
Proposed System	2	Yes	0.90	99.5

6 Conclusion

In this paper, an adaptive tracking technique based on P&O and IC MPPT for standalone solar PV systems is discussed. The adaptive technique is based on the sector location of the solar PV curve. The P-V characteristic curve is divided into four and six operational regions based on a new combined irradiance curve and variable step-size control system is implemented depending on the region of operation. The proposed system has been successfully built and evaluated using a solar development system. The measured results also have been verified with theory and simulation based on the modified control specification of the laboratory scale solar development system implemented together with the MPPT algorithm in the C2000 MCU. The tests have been performed under UIC and PSC. The results show improved steady state operation and settling time at MPP for UIC and PSC and satisfactorily tracks the GMPP under PSC. The system tracking efficiency of the proposed system is over 10 % greater than the conventional system for all techniques. Further study would focus on building a grid-connected system and analysing the MPPT and system performance.

References

1. BP Energy Economics, 2018 BP Energy Outlook p. 125 (2018)
2. Department of Energy & Climate Change, (July 2011) (2011)
3. T.E. Tawil, J.F. Charpentier, M. Benbouzid, *Renewable Energy* **115**, 1134 (2018)
4. L. Sheng, Z. Zhou, J. Charpentier, M. Benbouzid, *Renewable Energy* **103**, 286 (2017)
5. N. Kumar Moluguri, C. Rama Murthy, V. Harshavardhan, *Materials Today: Proceedings* **3**(10), 3637 (2016)
6. E. Kabir, P. Kumar, S. Kumar, A.A. Adelodun, K.H. Kim, *Renewable and Sustainable Energy Reviews* **82**, 894 (2018)
7. K.H. Solangi, M.R. Islam, R. Saidur, N.A. Rahim, H. Fayaz, *Renewable and Sustainable Energy Reviews* **15**, 2149 (2011)
8. D.C. Huynh, M.W. Dunnigan, *IEEE Transactions on Sustainable Energy* **7**(4), 1421 (2016)
9. Giulia GRANCINI, *Photoniques* pp. 24–31 (2019)
10. S. Racharla, .K. Rajan, K. Rajan, *International Journal of Sustainable Engineering* **10**(2), 72 (2017)
11. S.S. Eldin, M. Abd-Elhady, H. Kandil, *Renewable Energy* **85**, 228 (2016)
12. C.W.T.C.W. Tan, T. Green, C. Hernandez-Aramburo, 2008 IEEE 2nd International Power and Energy Conference (PECon 08), 237 (2008)
13. M.A. Ramli, S. Twaha, K. Ishaque, Y.A. Al-Turki, *Renewable and Sustainable Energy Reviews* **67**, 144 (2017)
14. K. Ishaque, Z. Salam, *Renewable and Sustainable Energy Reviews* (2013)
15. Y.H. Liu, S.C. Huang, J.W. Huang, W.C. Liang, *IEEE Transactions on Energy Conversion* **27**(4), 1027 (2012)
16. M.A.S. Masoum, H. Dehbonei, E.F. Fuchs, *IEEE TRANSACTIONS ON ENERGY CONVERSION* **17**(May), 514 (2014)
17. C.R. Algarín, J.T. Giraldo, O.R. Álvarez, *Energies* **10**(12) (2017)
18. M.T. Penella, M. Gasulla, *International Journal of Photoenergy* **2014**(1), 1 (2014)
19. H. Islam, S. Mekhilef, N. Shah, T. Soon, M. Seyedmahmousian, B. Horan, A. Stojcevski, *Energies* **11**(2), 365 (2018)
20. I. Houssamo, F. Locment, M. Sechilariu, *Renewable Energy* **35**(10), 2381 (2010)
21. L. Piegari, R. Rizzo, I. Spina, P. Tricoli, *Energies* **8**(5), 3418 (2015)
22. C. Jaen, C. Moyano, X. Santacruz, J. Pou, A. Arias, *Proceedings of the 15th IEEE International Conference on Electronics, Circuits and Systems, ICECS 2008* pp. 1099–1102 (2008)
23. R.I. Putri, S. Wibowo, M. Rifa'i, in *Energy Procedia*, vol. 68 (2015), vol. 68, pp. 22–30
24. K. Visweswara, *Energy Procedia* **54**, 11 (2014)
25. A. Akbar Ghassami, S. Mohammad Sadeghzadeh, A. Soleimani, *Electrical Power and Energy Systems* **53**, 237 (2013)

26. V. Ganesh, C.B. Jadhav, Y.R. Choudhari, O.N. Kate, V.S. Rajguru, 2017 7th International Conference on Power Systems (ICPS) pp. 7–12 (2017)
27. G. Yükses, A.N. Mete, 2017 10th International Conference on Electrical and Electronics Engineering (ELECO) pp. 949–953 (2017)
28. I.F. Anya, C. Saha, H. Ahmed, N. Huda, R. Sujan, in *Modern MPPT Techniques for Photovoltaic Energy Systems*, ed. by A.A.Y. Eltamaly, Ali M., 1st edn. (Springer International Publishing, Switzerland, 2019), chap. 8
29. K. Lappalainen, S. Valkealahti, *Applied Energy* **190**, 902 (2017)
30. M.Z. Ramli, Z. Salam, *Renewable Energy* **139**, 1336 (2019)
31. R. Alonso, P. Ibáñez, V. Martínez, E. Román, A. Sanz, 13th European Conference on Power Electronics and Applications, 2009. EPE '09. pp. 1–8 (2009)
32. K. Sundareswaran, S. Palani, V. Vigneshkumar, *IET Renewable Power Generation* **9**(7), 757 (2015)
33. K.L. Lian, J.H. Jhang, I.S. Tian, *IEEE Journal of Photovoltaics* **4**(2), 626 (2014)
34. L.L. Jiang, D. Nayanasiri, D.L. Maskell, D. Vilathgamuwa, *Renewable Energy* **76**, 53 (2015)
35. B. Benlahbib, N. Bouarroudj, S. Mekhilef, T. Abdelkrim, A. Lakhdari, F. Bouchafaa, *ELEKTRONIKA IR ELEKTROTEHNIKA* pp. 38–44 (2018)
36. K. Sundareswaran, V. Vignesh kumar, S. Palani, *Renewable Energy* **75**, 308 (2015)
37. N. Abdullahi, C. Saha, R. Jinks, *Journal of Renewable and Sustainable Energy* **033501**, 1 (2017)
38. A. Ramyar, H. Iman-Eini, S. Farhangi, *IEEE Transactions on Industrial Electronics* **64**(4), 2855 (2017)
39. N. Femia, G. Petrone, G. Spagnuolo, M. Vitelli, *Power Electronics and Control Techniques for Maximum Energy Harvesting in Photovoltaic Systems*, 1st edn. (CRC Press, 2013)
40. R.W. Erickson, D. Maksimovic, *Fundamentals of Power Electronics*, 2nd edn. (Springer, 2001)
41. F.L. Luo, H. Ye, *Power Electronics*, *IEEE Transactions on* **22**(1), 69 (2007)
42. S. Ramani, S.K. Kollimalla, B. Arundhati, 2017 International Conference on Circuit, Power and Computing Technologies (ICCPCT) pp. 1–7 (2017)
43. K. Jha, R. Dahiya, in *Numerical Optimization in Engineering and Sciences. Advances in Intelligent Systems and Computing* (Springer International Publishing, Singapore, 2020)
44. J. Ahmed, Z. Salam, *IEEE Transactions on Industrial Informatics* **11**(6), 1378 (2015)
45. B.N. Alajmi, K.H. Ahmed, S.J. Finney, B.W. Williams, *IEEE Transactions on Industrial Electronics* **60**(4), 1596 (2013)
46. C. Manickam, G.R. Raman, G.P. Raman, S.I. Ganesan, C. Nagamani, *IEEE Transactions on Industrial Electronics* **63**(10), 6097 (2016)